Heliyon 7 (2021) e07585

Contents lists available at ScienceDirect

Heliyon

journal homepage: www.cell.com/heliyon

Research article

Corrosion assessment of metals in bioethanol-gasoline blends using electrochemical impedance spectroscopy

Libia M. Baena [a,*], Ferley A. Vásquez [b], Jorge A. Calderón [b]

[a] Grupo de Calidad, Metrología y Producción, Instituto Tecnológico Metropolitano ITM, Medellín, Colombia
[b] Centro de Investigación, Innovación y Desarrollo de Materiales-CIDEMAT, Universidad de Antioquia, Medellín, Colombia

ARTICLE INFO

Keywords:
Corrosion
Electrochemical techniques
Bioethanol
Metals

ABSTRACT

Due to the increased use of environmentally friendly fuels, it becomes imperative to evaluate the impact of biofuels on the performance of materials used in auto parts. The corrosive effects of biofuels are important in terms of durability of auto-parts since there is an evidence of the increasing deterioration in automobile parts with the long-term use of biofuels. In this research, the behavior of metals, used in the manufacturing of auto parts, in pure bioethanol (E100) and bioethanol-gasoline blends with 30% (E30), 50% (E50), and 85% (E85) of ethanol content were evaluated. Electrochemical impedance Spectroscopy (EIS) curves were done under static conditions at 45 °C. The metallic materials evaluated were stainless steel, tin, carbon steel and copper. The EIS diagrams showed two capacitive arcs for all materials. The high frequency arc was related to the dielectric response of the fuel blends, while the second one shows the characteristics and activity of the metal/fuel interface. According to the transfer resistance (Rt) obtained from the second arc of the EIS measurements, copper and carbon steel exhibited corrosion susceptibility in all fuel blends, while stainless steel and tin showed good anticorrosion behavior by showing high Rt values. The highest charge transfer resistance was showed by tin, followed by stainless steel, carbon steel and copper. Except for carbon steel and copper, the other set samples were compatible with the evaluated blends.

1. Introduction

One of the main biofuel used to replace gasoline in the transport sector is bioethanol. The use of biofuels brings some benefits such as reduced demand for oil and polluting emissions, vehicle engine performance and development of rural sectors [1]. Also, have a huge source of production and manufacturing processes simple. However, these biofuels have a major disadvantage associated with materials compatibility. The introduction of alternative fuels often creates corrosion problems; their physicochemical properties are different from conventional fuel [2]. The corrosiveness of ethanol may be associated with its affinity with the water, which is oxidized to acetic acid which lowers the pH of the fuel as opposed to the electrical conductivity gas present [3]. The miscibility of alcohol with water and its subsequent separation can also accelerate corrosion problems. In addition to the increased probability of attack due to the presence of water, there is also the presence of organic acids related to the alcohol combustion process. Metallic and non-metallic materials can suffer deterioration due to the use of fuels mixed with ethanol, among these we can mention steel, aluminum, zinc, copper, rubber, and polymeric components [2]. In general, the impact of metallic corrosion on components of the fuel system in vehicles because of oxygenated fuels, causes malfunction and premature failure, since corrosion on electrical connections reduces electrical conductivity and acts as a source of wear and abrasion among auto parts, leading to significant financial repercussions. Different studies have been carried out to address the issue related to the compatibility of metals in ethanol media, such as pitting [4], stress corrosion [5, 6], electrochemical tests [7], immersion tests of long duration static [3], etc. It has been reported that ethanol percentages of 30, 85, and 100% do not cause corrosion in stainless steel AISI 304 [8]. To prevent these problems of corrosion of metallic materials in contact with ethanol, have been proposed some anti-corrosion coatings and corrosion inhibitors [9]. In general, the recommended upper limit of ethanol in gasoline blends is up to 10% [10]. An increase the ethanol concentration to 20% or more can cause corrosive effects unpredictable aluminum and its alloys [11]. In addition, the high temperature conditions in the engines idling vehicles can change some characteristics of blends gasoline-ethanol and cause corrosion in metallic materials [12].

* Corresponding author.
E-mail address: libiabaena@itm.edu.co (L.M. Baena).

https://doi.org/10.1016/j.heliyon.2021.e07585
Received 3 February 2021; Received in revised form 31 May 2021; Accepted 12 July 2021

Table 1. Review table including corrosion type, corrosion mechanism, aggressive agent, control method, and corrosion assessment technique for pipelines in carbon steel and some carbon, magnesium, lead and aluminum auto parts in contact with gasoline-ethanol blends.

Medium or fluid	Metallic structure or material	Corrosion morphotype	Corrosion mechanisms	Aggressive agent	Control method	Evaluation technique	Ref
Oil and gas	Pipelines (carbon steel)	• General corrosion • Localized corrosion	• $Fe + CO_2 + H_2O \rightarrow FeCO_3 + H_2$ • $2H^+ + 2e^- \rightarrow H_2$ • $2H_2CO_3 + 2e^- \rightarrow H_2 + 2HCO_3^-$ • $(2HCO_3)^- + 2e^- \rightarrow H_2 + 2CO_3^{-2}$	CO_2	Inhibitors corrosion: • Amides, imidazoline. • Salts of nitrogen (molecules with carboxylic acids) • Amines, amides.	• Visual examination. • Rate of penetration statically (the depth of the deepest pit on the surface of a metal is the upper tail of the distribution of depths of all pits on that metal). Extreme value statistics (EVS) for characterization of the well depth distribution. • Electrochemical methods. • Use of metal coupons (Uniform corrosion: determination of mass loss and corrosion rate calculation. Corrosion pitting: measure of the depth of the deepest well).	[13, 15, 16, 17, 18, 19, 20, 21]
		• Acid corrosion	• $Fe + H_2S \rightarrow FeS + H_2$ • $Fe(OH)^+ + H^+ + OH^- \rightarrow FeS + 2H_2O$	H_2S			[13, 17, 20, 21, 22]
		• Top of line corrosion (TOLC)	• $Fe + H_2S \rightarrow FeS + H_2$ • $Fe + CO_2 + H_2O \rightarrow FeCO_3 + H_2$ • $Fe + 2HAc \rightarrow Fe^{2+} + H_2 + 2Ac^-$ • $2Fe + O_2 + 4H^+ \rightarrow 2Fe^{2+} + H_2 + 2H_2O$	• Flow regime • Gas flow rate • Acid gasses • Temperature • CO_2 partial pressure in gas			[13, 14, 20, 21]
		• Microbiologically influenced corrosión (MIC)	• (IOB):$4FeCO_3 + O_2 + 6H_2O \rightarrow 4Fe(OH)_3 + 4CO_2$ • (SRB):$4Fe + SO_4^{-2} + 4H_2O \rightarrow FeS + 3Fe(OH)_2 + 2OH^-$	• Sulfates • Bacteria • Ph • Flow rate • Temperature • Salinity	• Physical cleaning • Mechanical modifications. • Use of biocides • Creation of a diffusion barrier to corrosion products that prevent the dissolution of the metal and the consumption of oxygen due to the presence of aerobic microorganisms inside the biofilm.		[20, 21, 23, 24]
Gasoline-Bioethanol blends	Magnesium, lead and aluminum	• Dry corrosion	• Ethanol belongs to the protonic solvents (they have a high tendency to receive or give up protons) and its dissociation is represented according to the following equilibrium: $2CH_3CH_2OH \leftrightarrow CH_3CH_2OH_2^+ + CH_3CH_2O^-$ • Cathodic reduction of ethanol in the presence of adsorbed oxygen and a metal: $\frac{1}{2}O_2 + C_2H_5OH + 2e^- \rightarrow OH_{ads}^- + C_2H_5O_{ads}^-$ • The two electrons are supplied by the anodic solution of the metal: $M \rightarrow M^{2+} + 2e^-$ • The surface of the metal is quickly covered by ethoxide, thus giving the following anodic reaction: $MM(OC_2H_5)^-_{ads} \rightarrow M(MOC_2H_5)_{ads} + e^-$ • The intermediate species (MOC2H5) ads is more stable than its analog species MeOH ads. The oxidation of (MOC2H5) ads and the activation of the metal surface in ethanol proceeds according to the following reaction: $M(MOC_2H_5)_{ads} \rightarrow M(OC_2H_5)_{ads} + M^{2+}{}_{sol} + 2e^-$	• Ethanol • Water	Inhibitors corrosion: • Ethanolamine • Diethanolamine • Triethanolamine			[20, 21, 25, 26, 27, 28, 29, 30]
	Fuel tank (Carbon steel)	• General Corrosion • Corrosion pitting	• $xM + yH_2O \rightarrow MxOy + yH_2$ • $xM + 1/2yO_2 \rightarrow M_XO_Y$ • $M_XO_Y + H_2O \rightarrow M_X(OH)_Y + OH^-$	The aqueous phase undergoes a change in its structure that depends on: • Atmospheric pressure			[20, 21, 28, 31, 32]

(*continued on next page*)

Table 1 (*continued*)

Medium or fluid	Metallic structure or material	Corrosion morphotype	Corrosion mechanisms	Aggressive agent	Control method	Evaluation technique	Ref
				• Liquid temperature • Amount of polar components in gasoline (aromatic substances) Due to an exothermic interactions with water, ethanol Is distributed in the aqueous phase, which becomes ethanol saturated with water, compounds contaminants and aromatic hydrocarbons.			

Similar to the deterioration by corrosion of auto parts in contact with biofuels, in the oil and gas industry problems due to electrochemical corrosion have also been evidenced, especially in carbon steel pipes [13]. It has been reported that the most common types of corrosion in gas and fuel pipes are [13]:

- *CO_2 corrosion*: CO_2 corrosion is one of the most frequent in pipelines producing localized or generalized attack.
- *H_2S corrosion*: the presence of this weak acid gas produces different corrosion mechanisms in the pipes that transport hydrocarbons and gases. In the case of carbon steel, the dissociation of H_2S in the aqueous phase produces a greater amount of H +, in this way it can increase the speed of anodic dissolution of the steel and the cathodic reduction by trapping electrons.
- *Microbiologically influenced corrosion (MIC):* The bacteria that most promote this type of corrosion are sulfate reducing bacteria (SRB), acid producing bacteria (APB), iron reducing and oxidizing bacteria (IRB) and (IOB).
- *Top of line corrosion (TOLC):* TOLC corrosion is associated with the condensation of water in the upper part of the interior of the pipes. It commonly occurs in pipes that transport wet gases with sweet hydrocarbons [14].

Table 1 shows the types of corrosion, mechanisms, control methods and corrosion evaluation techniques for pipelines and some metallic materials in contact with gasoline-ethanol mixtures. According to the literature review there is some lack of knowledge about the performance against corrosion of metals used in auto parts that are in direct contact with gasoline-ethanol blends with high ethanol content (>12%), which is the aim of this work. Besides, the use of electrochemical techniques for the evaluation of the metal corrosion in gasoline-ethanol blends as electrolyte is very limited because of the low conductivity of the gasoline-ethanol blends, which can mask corrosion processes at the metal/electrolyte interface. So, in this work, the use of EIS measurements to evaluation of the corrosion susceptibility of metals immersed in gasoline-ethanol blends is also explored.

2. Experimental procedure

2.1. Metal specimens

Metallic samples studied were prepared according to the procedures described by ASTM G1-90 and ASTM G31-72 standards. The area of each specimen was measured before exposure to test fluids, providing a benchmark for comparison. The most representative materials of vehicle metal auto-parts were chosen, including stainless steel 314 (SS), AISI SAE 1005 carbon steel (CS), electrolytic copper 99% (Cu) and pure tin (99%). Before the exposure, samples were polished with sandpaper 600 grit. Then, they were washed and degreased in water and ethanol.

2.2. Test fuels

The fuel used for the tests were pure bioethanol (E100) and gasoline-ethanol blends as 30% ethanol and 70% gasoline (E30), 50% ethanol and 50% gasoline (E50) and 85% ethanol and 15% gasoline (E85). Chemical composition of bioethanol (from sugar-cane) used was: 99% ethanol, 0.002% acetic acid, 0.5% moisture, 0.5% diethylphthalate, and 0.1% cyclohexane.

2.3. Electrochemical tests

In order to evaluate the corrosion resistance properties of the metal under study and the corrosivity of the bioethanol-gasoline blends, EIS measurements at different immersion times were carried out in an electrochemical cell of two identical working electrodes. Gasoline-ethanol blends are media with high resistivity, which makes it

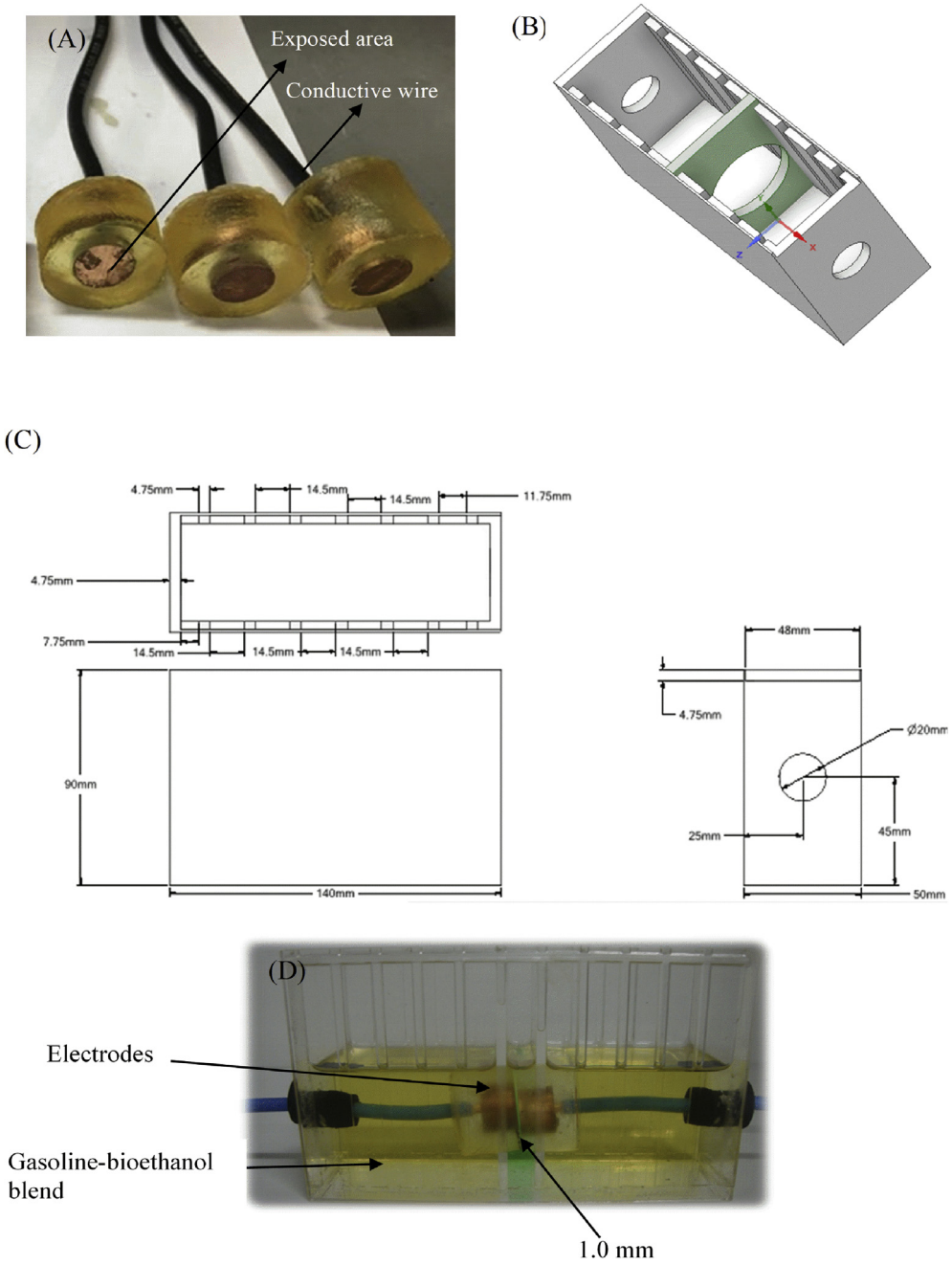

Figure 1. Electrochemical cell used in the EIS measurements to evaluate the corrosiveness of the ethanol-gasoline blends. (A) working electrodes; (B) 3D drawing of the electrochemical cell; (C) drawing of the electrochemical cell; (D) electrochemical cell assembly with working electrodes and gasoline-ethanol blends as electrolyte.

significantly difficult to obtain electrochemical measurements [33]. For that reason, in this work the cell configuration with two identical working electrodes positioned one in front of the other was used, which is usually useful to evaluate the electrochemical response of the metal/electrolyte interface in highly resistive media [33]. For the manufacture of the working electrodes, circular metal samples were taken with an exposed area of 2.0 cm^2, see Figure 1A. Then, electrodes were welded to a conductive wire and finally they were embedded in epoxy resin as an insulating material. The surface of the working electrodes was polished with SiC paper to grade 1000 and then degreased with ethanol and acetone. An acrylic box with internal guides, where plates with a circular opening of 4 cm^2 were inserted, was used as electrochemical cell. The electrodes were placed into the circular openings, in this way a separation of 1 mm between the electrodes was guaranteed (see details of cell assembly in Figure 1 B-D).

The resistance of the first capacitive arc of the Nyquist diagrams of EIS measurements of the metallic materials under study follows Ohm's law, i.e., the resistance is directly proportional to the separation between the working electrodes, that because the first capacitive loop observed in the EIS diagrams is associated with the dielectric response of the gasoline-bioethanol blends [34]. Therefore, the distance of 1 mm between electrodes allowed to overcome problems with the data acquisition and with the reliability of the EIS measurements, due to the low conductivity of the gasoline-ethanol blends as electrolyte [8, 9]. Figure 1D shows a real photo of the cell and the arrangement of the electrodes for electrochemical impedance measurements. In said cell scheme, the loss due to ohmic drop is eliminated since a reference electrode is not used as the third element of the circuit. In this way, the output of the potentiostat for the working electrode and the reference electrode are short-circuited at one of the electrodes and the output of the counter-potentiostat electrode

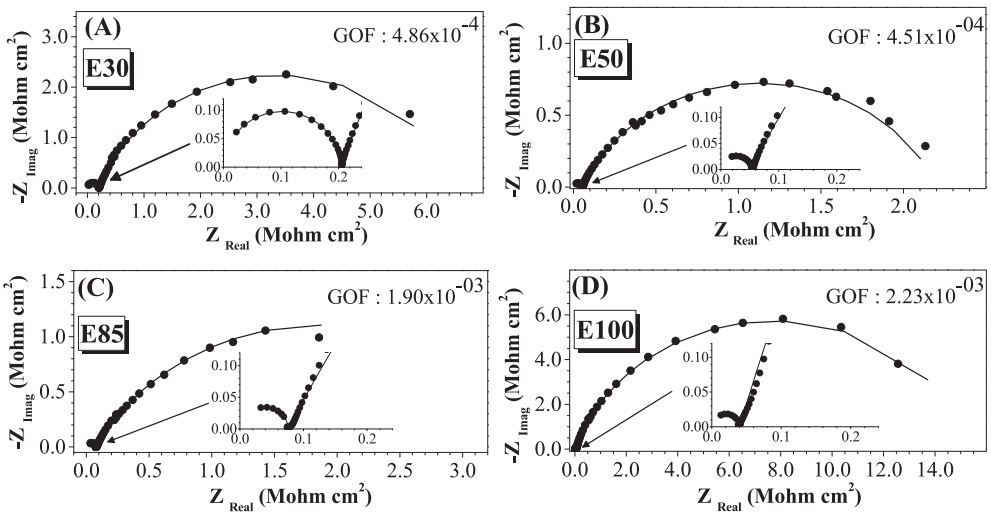

Figure 2. Impedance diagrams obtained of Copper at 30 days of immersion in (A) E30, (B) E50, (C) E85, (D) E100. Experimental values (dots) and fitted profile (lines) with goodness of Fit value (GOF).

is connected to the other working electrode. In this way the impedance response of the system is the impedance of two identical surfaces. The response signal must be divided by 2 to obtain the conventional electrochemical impedance measurement. E30, E50, E85 and E100 blends was used as electrolyte at 45 °C. EIS measurements were performed at immersion times of 0, 2, 8, 15 and 30 days, using a 302 Auto lab PGSTAT Potentiostat controlled by NOVA software. EIS measurements were carried out at open circuit potential in a frequency range between 100 kHz to 0.5 mHz with a sinusoidal perturbation amplitude of 50 mV. Before all measurements, several EIS measurements were performed at different perturbation amplitudes: 10mV, 15mV, 20mV, 30mV and 50 mV and all EIS curves overlapped (Nyquist plots were the same), indicating that the electrochemical system was lineal at the OCP. Due to the low conductivity of the electrolytes, which were bioethanol and gasoline-bioethanol blends, the highest amplitude perturbation (50 mV) was necessary in order to obtain the lowest signal-to-noise (S/N) ratio during the measurements and to achieve low dispersion in the EIS plots.

The electrochemical impedance curves allow to obtain information on the electrical conductivity of the mixture and its aggressiveness. These results will allow us to calculate the charge transfer resistance (R_t), which is a parameter that corresponds to the oxidation processes in metals, and it's directly related to the resistance to corrosion of each metal. In order to determine the corrosion current density (I_{corr}) of the metallic materials immersed in the fuel blends, the values of charge transfer resistance (R_t) were taken from the second arc of the EIS diagrams. I_{corr} was calculated following Eq. (1) [35]:

$$I_{corr} = \frac{B}{R_t} \tag{1}$$

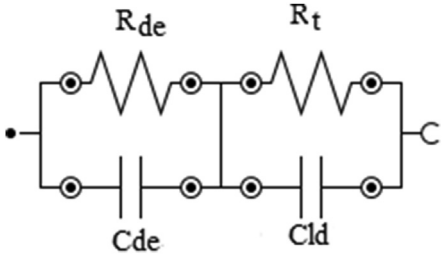

Figure 3. Equivalent electrical circuit (RC) (RC) for the impedance response for all metals immersed in gasoline-ethanol blends.

where B is the Stern-Geary's constant and R_t is the charge transfer resistance [36]. B was calculated according to Eq. (2):

$$B = \frac{\beta_a \beta_c}{2.3(\beta_a + \beta_c)} \tag{2}$$

where the β_a and β_c are anodic and cathodic Tafel slopes, respectively. The low conductivity of the electrolyte (bioethanol-gasoline blends) makes difficult to obtain accurate polarization curves and reliable values of Tafel constants (β_a and β_c). According to Stern [37], when Tafel constants are unknown the value of 0.1 V for $|\beta_a|$ and $|\beta_c|$ can be used and a small error that not exceed a factor of 2, comparable to experimental error, would be assumed. The corrosion rate in millimeters per year (mm/y) was calculated following Eq. (3) [35]:

$$CR = K_1 \frac{I_{corr}}{\rho} EW \tag{3}$$

where K_1 is a constant equal to 3.27×10^{-3} (mm g/μA cm yr), I_{corr} is the corrosion current density calculated according to Eq. (1) and EW is the equivalent weight of the metal or alloy (atomic weight/n° electrons) and ρ (g/cm^3) is the density of the material.

The surface of metals specimens was characterized by Scanning Electron Microscopy (SEM) and X-ray dispersive energy spectroscopy (EDS). The equipment used was a scanning electron microscope JEOL model JSM 6490 LV, with secondary and backscattered electron detector, an acceleration voltage of 20 kV and a working distance of 10 mm.

3. Results and discussion

3.1. Electrochemical impedance spectroscopy measurements

Figure 2 presents the impedance diagrams (Nyquist plots) of copper immersed for 30 days in all the blends. It can be seen that these diagrams are constituted by two delimited capacitive arcs. It was observed that the characteristic frequencies of the first arc of the EIS diagrams, for all the metals evaluated, were ranged from 40 kHz to10 kHz, and evidenced capacitance values of the order of 10^{-12} F cm^{-2}. These capacitance values are not common for the electric double layer; therefore, they might be related to the dielectric response of the gasoline-bioethanol blends as electrolytes. The characteristic frequency of the second arc in all tested metallic materials is ranged between 7 and 0.5 mHz, which gives capacitances of 40–5 μF cm^{-2} order. These values of capacitances are more commonly found for electrical double layer of the metal/

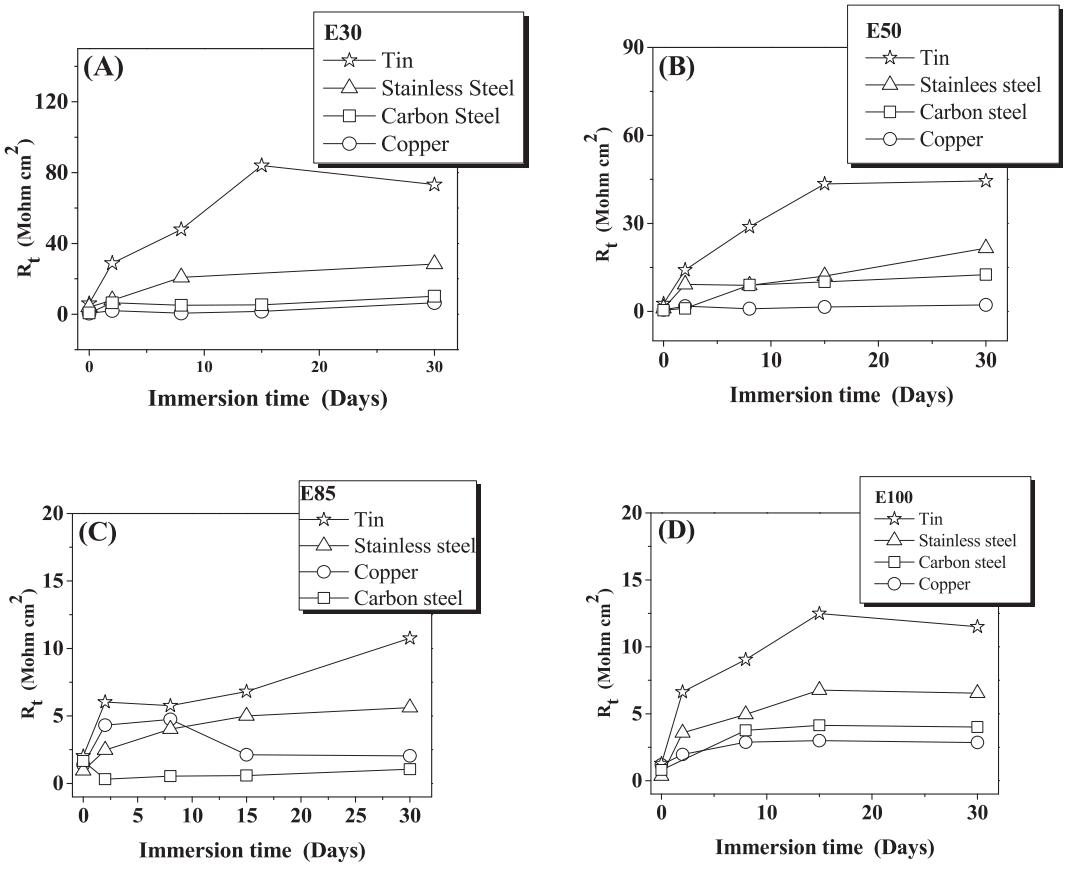

Figure 4. Variation of the *Rt* of the metals exposed to gasoline-ethanol blends at different immersion times. (A) E30, (B) E50, (C) E85, (D) E100.

electrolyte interfaces. This result suggests that the second capacitive arc at low frequencies can be associated with the corrosion processes happening on the surface of metals immersed in the gasoline-ethanol blends. The experimental Nyquist plots of the EIS measurements performed to CS, SS, and Sn immersed in the blends at different times of immersion (not presented in this paper) showed similar characteristics to those exhibited by copper. According to the observation that the second capacitive loop displayed in the EIS diagrams is associated with the corrosion processes of the metals, the charge transfer resistance (*Rt*) of the corrosion process of each metal could be obtained from the impedance of that loop. *Rt* values were determined by fitting of the EIS diagrams with the equivalent electrical circuit showed in Figure 3. The impedance response of the electrochemical system for all metals immersed in blends of gasoline-bioethanol can be the same as the response of the electric circuit constituted by two parallel RC circuits linked in series, as shown in Figure 3. According to the results given by

Table 2. Electrical parameters of metals extracted from the second loop of impedance diagrams.

Parameter		Cdl (μF cm^{-2})				Rt (Mohm cm^2)				Corrosion Rate (mm year^{-1})			
Metal		Cu	CS	SS	Sn	Cu	CS	SS	Sn	Cu	CS	SS	Sn
Blend	Time (days)												
E30	2	0.68	48.56	11.50	2.11	1.97	6.44	7.99	28.82	2.55×10^{-4}	3.91×10^{-5}	2.79×10^{-5}	2.00×10^{-5}
	8	17.5	10.53	5.17	1.33	0.59	5.08	20.83	47.91	8.53×10^{-4}	4.95×10^{-5}	1.07×10^{-5}	1.20×10^{-5}
	15	7.2	5.95	–	0.78	1.67	5.37	–	83.97	3.01×10^{-4}	4.69×10^{-5}	–	0.69×10^{-5}
	30	9.43	7.09	9.73	0.86	6.50	10.22	28.35	73.26	0.77×10^{-4}	2.46×10^{-5}	0.79×10^{-5}	0.79×10^{-5}
E50	2	18.49	30.51	30.39	2.09	1.81	1.02	9.2	14.16	2.78×10^{-4}	24.70×10^{-5}	2.42×10^{-5}	4.07×10^{-5}
	8	6.11	12.61	28.21	2.36	0.93	9.01	8.87	28.81	5.41×10^{-4}	2.79×10^{-5}	2.51×10^{-5}	2.00×10^{-5}
	15	4.37	7.68	22.42	1.55	1.5	10.11	12.07	43.45	3.36×10^{-4}	2.49×10^{-5}	1.85×10^{-5}	1.33×10^{-5}
	30	7.9	3.56	13.96	1.53	2.25	12.52	21.59	44.51	2.24×10^{-4}	2.01×10^{-5}	1.03×10^{-5}	1.30×10^{-5}
E85	2	6.56	14.64	21.91	2.51	1.3	1.68	0.93	2.02	3.87×10^{-4}	1.50×10^{-4}	24.0×10^{-5}	28.6×10^{-5}
	8	6.11	18.8	15.02	1.59	4.74	0.53	4.02	5.75	1.06×10^{-4}	4.75×10^{-4}	5.54×10^{-5}	10.0×10^{-5}
	15	21.43	9.77	13.31	1.67	2.11	0.58	4.99	6.8	2.39×10^{-4}	4.34×10^{-4}	4.47×10^{-5}	8.48×10^{-5}
	30	51.84	4.19	20.25	1.89	2.04	1.05	5.61	10.76	2.47×10^{-4}	2.40×10^{-4}	3.97×10^{-5}	5.36×10^{-5}
E100	2	5.88	91.25	90.37	3.52	1.19	0.79	0.36	1.28	4.23×10^{-4}	31.8×10^{-5}	61.9×10^{-5}	45.1×10^{-5}
	8	8.72	19.38	64.78	3.11	2.87	3.76	4.95	9.05	1.75×10^{-4}	6.69×10^{-5}	4.50×10^{-5}	6.37×10^{-5}
	15	8.32	16.94	48.09	5.12	2.98	4.13	6.76	12.49	1.69×10^{-4}	6.09×10^{-5}	3.30×10^{-5}	4.62×10^{-5}
	30	7.43	13.84	48.41	5.59	2.85	4.01	6.53	11.5	1.77×10^{-4}	6.27×10^{-5}	3.41×10^{-5}	5.02×10^{-5}

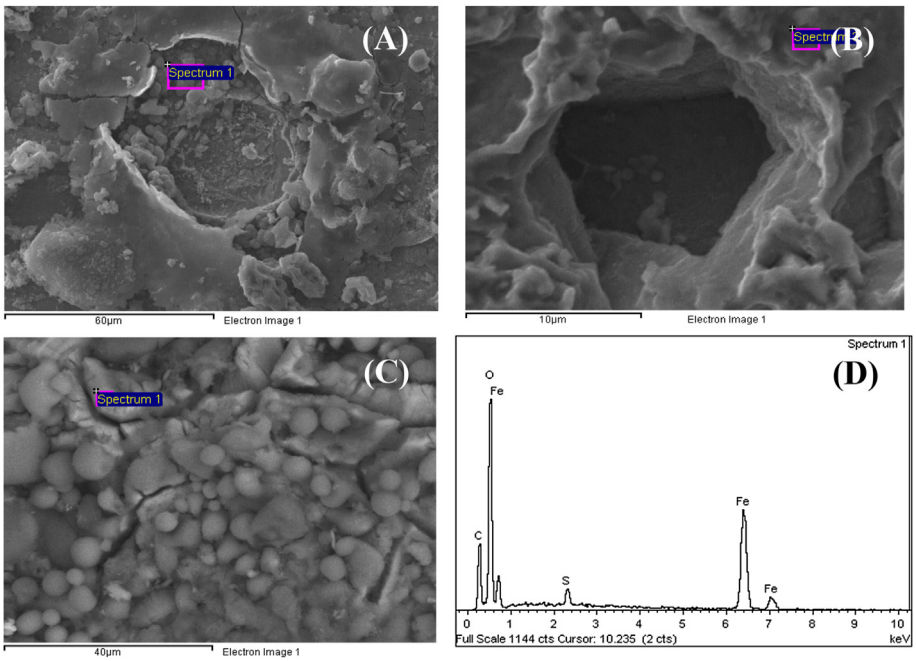

Figure 5. Characterization of the surface of carbon steel immersed in E30 for 90 days at 45 °C. (A–C) SEM images, (D) EDS.

Table 3. EDS quantification of elements on carbon steel surface, immersed in E30 for 90 days at 45 °C.

Element	App	Intensity	Weight%	Atomic%
C K	34.33	0.63	24.24 (88)	37.27
O K	99.11	0.97	45.33 (80)	52.32
S K	2.82	0.90	1.39 (12)	0.80
Fe K	54.68	0.84	29.04 (61)	9.60

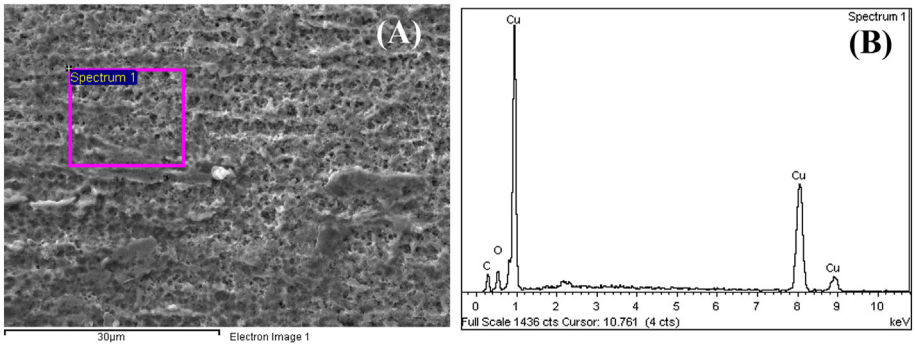

Figure 6. Characterization of the surface of cooper immersed in E30 for 90 days at 45 °C. (A) SEM images, (B) EDS.

Table 4. EDS quantification of elements on cooper surface, immersed in E30 for 90 days at 45 °C.

Element	App	Intensity	Weight%	Atomic%
C K	12.45	0.34	15.39 (120)	43.82
O K	13.57	0.87	6.66 (52)	14.24
Cu K	167.91	0.93	77.94 (120)	41.94

EIS in time, the tested metallic materials showed high *Rt* of the order of megaohms, and they can be classified according to the susceptibility to corrosion of those metals in E30 and E50 from the highest to the lowest, as follows: copper > carbon steel > stainless steel > tin. In E85 as follows: carbon steel > copper > tin > stainless steel. In E100 as follows: copper > carbon steel > tin > stainless steel.

Figure 4 illustrates the variation of the *Rt* of the second arc of EIS measurements as function of the immersion time for all the metallic material in all fuel blends. It was observed that *Rt* values for stainless steel increase during first 30 days of immersion in E30 from 3.8 to 22 MOhm, in E50 from 1.0 to 21.5 MOhm, in E85 from 0.9 to 5.6 MOhm, and in E100 from 0.3 to 6.5 MOhm. On the other hand, the capacitance

values of the stainless steel corresponding to the second loop of the EIS diagrams, decreased significantly after 30 days of immersion in E30 from 45.7 to 14.2 μF cm^{-2}, in E50 from 30.3 to 13.9 μF cm^{-2}, in E85 from 21.9 to 20.2 μF cm^{-2} and in E100 from 90.3 to 48.4 μF cm^{-2}. These values are of the order of 1×10^{-5} F, typical values of an electrical double layer capacitance. Tin presented a similar behavior to stainless steel, the *Rt* of this material increased during the first 30 days of immersion in E30 from 6.0 to 73.2 MOhm, in E50 from 2.6 to 44.5, in E85 from 2.0 to 10.76, and in E100 from 1.2 to 11.5 MOhm. The tin capacitance values corresponding to the second loop of the EIS diagrams also decreased after 30 days of immersion in E30 from 2.1 to 0.8 μF cm^{-2}, in E50 from 2.0 to 1.5 μF cm^{-2}, in E85 from 2.5 to 1.8 μF cm^{-2}, except in the E100 mix where the capacitance increases slightly from 3.5 to 5.5 μF cm^{-2}. The *Rt* values observed for copper show slight increases during the first 30 days of immersion in E30 from 0.5 to 6.5 MOhm, in E50 from 0.5 to 2.25, in E85 from 1.3 to 2.0, and in E100 from 1.1 to 2.8 MOhm. The copper capacitance values corresponding to the second loop observed in the EIS diagrams, increased after 30 days of immersion in E30 from 0.6 to 9.4 μF cm^{-2}, and in E85 from 6.5 to 51.8 μF cm^{-2}, while in E50 they decreased from 18.4 to 7.9 μF cm^{-2}, and in E100 from 5.8 to 7.4. μF cm^{-2}. The *Rt* values for carbon steel increase during the first 30 days of immersion in E30 from 0.6 to 10.2 MOhm, in E50 from 0.4 to 12.5, and E100 from 0.7 to 4.0 MOhm while the *Rt* decreases slightly in E85 from 1.6 to 1.0. Like stainless steel and tin, the capacitance values of carbon steel corresponding to the second loop observed in the EIS diagrams, decreased significantly after 30 days of immersion in E30 from 48.5 to 7.0 μF cm^{-2}, at E50 from 30.5 to 3.5 μF cm^{-2}, in E85 from 14.6 to 4.19 μF cm^{-2} and in E100 from 91.2 to 13.8 μF cm^{-2}. Note that as the ethanol concentration in the mixture increases, the *Rt* of the metals is lower, given the increase in conductivity of the medium. The increase in *Rt* of all the metals under evaluation during the immersion time (30 days) corresponds to a characteristic behavior of metallic materials, which form oxide layers on their surface when interacting with the test media. While the *Rt* values increased, the double-layer capacitance values for the metals under evaluation decreased, a result that can be associated with the creation of protective films on surface of metals [38]. It has been informed that the adsorption process on the metal surface it implies a decrease in the capacitance of the double layer [39]. The electrical parameters of the equivalent electrical circuit and the corrosion rate calculated using Eq. (3) of all metals immersed in the blends are presented in Table 2. Copper and carbon steel are the metals most likely to corrode in all mixtures, so they are not recommended for use in auto parts that are in contact with the test blends. Copper is used for electrical contacts in some auto parts, which when corroded could cause the electric fuel pump to malfunction. Carbon steel is part of the gas tank, and corroding can cause fuel leaks and subsequent vehicle failure.

3.2. Characterization of the oxide layers growing on the metallic materials exposed to blends

The characterization of the corrosion products formed on the surface of carbon steel and copper was carried out using SEM and analysis by EDS, in order to determine the chemical composition and quantify the elements present. Figure 5 shows the analysis of the surface of carbon steel immersed in E30 for 90 days at 45 °C. Figure 5A-B illustrates the holes after the eruption of bubbles created on the surface of the carbon steel, like a kind of "crater", which means that the creation of corrosion products began at the place where localized corrosion was evidenced. Figure 5C illustrates the image of the products formed inside the wells, which exhibits a cotton-like morphology, corresponding to the typical semi-crystalline goethite structure [40]. Figure 5C shows a typical morphology of the goethite, which is also frequently found in corrosion products of steels. Figure 5D and Table 3 presents the EDS analysis, where it can be observed that the main elements make up the corrosion products on surface of carbon steel are oxygen, carbon, and iron. The presence of 45.33% oxygen can be related with the formed of iron oxides, hydroxides, and oxyhydroxides, likewise, the presence of 24.24 % of C can be associated with the formation of iron carbonates [41]. The oxygen that influences the attack of the steel by corrosion and therefore the creation of iron oxides, is dissolved in the gasoline-bioethanol blends because these oxygenated fuels absorb water from the environment due to their high hygroscopic nature. It should be taken into account that water is an obligatory companion of gasoline-bioethanol blends, due to affinity that exists between both substances; ethanol is highly hygroscopic, that is, it has a high affinity for moisture and is completely soluble in water [31]. Therefore, open exposure to the environment during transport or storage tends to increase water content and the likely impacts of corrosion reactions [42]. Figure 6 presents an analysis of the surface of cooper immersed in E30 for 90 days at 45 °C. Figure 6A presents the morphology of the copper oxides formed on the metal surface as consequence of its immersion in the E30 blend. Figure 6B and Table 4 present the EDS analyzes performed on the copper surface to analyze the chemical composition of the corrosion products formed. This analysis showed the presence of O, C, and Cu, which may be related to the copper oxides and carbonates formed on the metal, such as cuprite (Cu2O) and tenorite (CuO).

4. Conclusions

Based on results of electrochemical impedance spectroscopy, in all blends of ethanol and gasoline, the most susceptible metals to corrosion were and carbon steel, therefore those metals are not recommended for auto-parts in contact with ethanol and gasoline blends. The case of copper may be less critical than steel because copper is used for electrical contacts, and not as a structural metal. The stainless steel and tin showed high values of Rt in all media therefore can be considered compatible metals blends of ethanol and gasoline, even at high concentrations of ethanol.

Declarations

Author contribution statement

Libia M. Baena: Conceived and designed the experiments; Performed the experiments; Analyzed and interpreted the data; Wrote the paper.

Ferley A. Vásquez: Analyzed and interpreted the data; Wrote the paper.

Jorge A. Calderón: Conceived and designed the experiments; Analyzed and interpreted the data; Contributed reagents, materials, analysis tools or data; Wrote the paper.

Funding statement

The author: Libia M. Baena was supported by the Instituto Tecnológico Metropolitano ITM. The authors: Jorge A. Calderón and Ferley A. Vásquez were supported by the Universidad de Antioquia.

Data availability statement

Data included in article/supplementary material/referenced in article.

Declaration of interests statement

The authors declare no conflict of interest.

Additional information

No additional information is available for this paper.

References

[1] L. Fulton, T. Howes, y J. Hardy, Biofuels for Transport: an International Perspective, International Energy Agency, Paris, France, 2004. Accedido: sep. 01, 2017. [En línea]. Disponible en: https://scholar.google.es/scholar?q=ulton,+L.,+T.+Howes,+and+J.+Hardy,+Biofuels+for+transport:+an+international+perspective.+2004:+OECD,+International+Energy+Agency.&hl=es&as_sdt=0.

[2] A. Agarwal, Biofuels (alcohols and biodiesel) applications as fuels for internal combustion engines, Prog. Energy Combust. Sci. (2007). Accedido: sep. 01, 2017. [En línea]. Disponible en: http://www.sciencedirect.com/science/article/pii/S0360128506000384.

[3] C. Berlanga-Labari, A. Albistur-Goñi, I. Barado-Pardo, Compatibility study of high density polyethylene with bioethanol–gasoline blends, Mater. Des. (2011). Accedido: sep. 01, 2017. [En línea]. Disponible en: http://www.sciencedirect.com/science/article/pii/S0261306910003924.

[4] X. Lou, P. Singh, Role of water, acetic acid and chloride on corrosion and pitting behaviour of carbon steel in fuel-grade ethanol, Corrosion Sci. (2010). Accedido: sep. 01, 2017. [En línea]. Disponible en: http://www.sciencedirect.com/science/article/pii/S0010938X10001848.

[5] N. Sridhar, K. Price, J. Buckingham, y J. Dante, Stress corrosion cracking of carbon steel in ethanol, Corrosion 62 (8) (2006) 687–702, ago.

[6] X. Lou, P.M. Singh, Phase angle analysis for stress corrosion cracking of carbon steel in fuel-grade ethanol: experiments and simulation, Electrochim. Acta 56 (4) (2011) 1835–1847, ene.

[7] F. Gui, N. Sridhar, Conducting electrochemical measurements in fuel-grade ethanol using microelectrodes, Corrosion (2010). Accedido: sep. 01, 2017. [En línea]. Disponible en: http://www.corrosionjournal.org.

[8] X. Nie, X. Li, y D. Northwood, Corrosion Behavior of metallic materials in ethanol-gasoline alternative fuels, Mater. Sci. Forum (2007). Accedido: sep. 01, 2017. [En línea]. Disponible en: https://www.scientific.net/MSF.546-549.1093.

[9] Corrosion in ethanol fuel powered cars: problems - google académico (accedido may 25, 2021), https://scholar.google.es/scholar?hl=es&as_sdt=0%2C5&q=Corrosion+in+Ethanol+Fuel+Powered+Cars%3A+Problems+and+Remedies&btnG=.

[10] A literature review based assessment on the impacts - google académico (accedido may 25, 2021), https://scholar.google.es/scholar?hl=es&as_sdt=0%2C5&q=A+Literature+Review+Based+Assessment+on+the+Impacts+of+a+20%25+Ethanol+Gasoline+Fuel+Blend+on+the+Australian+Vehicle+Fleet&btnG=.

[11] G. Mead, B. Jones, P. Steevens, y M. Timanus, The Effects of E20 on Metals Used in Automotive Fuel System Components, 2008. Accedido: sep. 28, 2017. [En línea]. Disponible en: http://cset.mnsu.edu/aet/facilities/msu_e20_metal_material_compatibility_study_2-22-08_final.pdf.

[12] Y. H. Yoo, I. J. Park, J. G. Kim, D. H. Kwak, y W. S. Ji, Corrosion characteristics of aluminum alloy in bio-ethanol blended gasoline fuel: Part 1. The corrosion properties of aluminum alloy in high temperature fuels, Fuel, vol. 90, n.o 3, pp. 1208-1214, mar. 2011.

[13] M. Askari, M. Aliofkhazraei, y S. Afroukhteh, A Comprehensive Review on Internal Corrosion and Cracking of Oil and Gas Pipelines, 2019.

[14] R. Nyborg, A. D-C, Undefined 2007, Top of Line Corrosion and Water Condensation Rates in Wet Gas Pipelines, *onepetro.Org*, 2007. Accedido: may 10, 2021. [En línea]. Disponible en: https://onepetro.org/NACECORR/proceedings-abstract/CORR07/All-CORR07/NACE-07555/127566.

[15] M.B. Kermani, A. Morshed, Carbon dioxide corrosion in oil and gas production - a compendium, Corrosion 59 (8) (2003) 659–683, ago.

[16] S. N.-C. science y undefined, Key Issues Related to Modelling of Internal Corrosion of Oil and Gas Pipelines–A Review, Elsevier, 2007. Accedido: jul. 17, 2019. [En línea]. Disponible en: https://www.sciencedirect.com/science/article/pii/S0010938X07001539.

[17] M. Askari, M. Aliofkhazraei, S. Ghaffari, y A. Hajizadeh, «Film former corrosion inhibitors for oil and gas pipelines - a technical review», Elsevier B.V. J. Nat. Gas Sci. Eng. 58 (2018) 92–114. oct. 01

[18] B.R. Ed, S.D. Jr, y S. Do, Corrosion Tests and Standards: Application and Interpretation, 1995.

[19] Statistical theory of extreme values and some practical applications: a emil julius gumbel - google libros (accedido may 17, 2021), https://books.google.com.co/books/about/Statistical_Theory_of_Extreme_Values_and.html?id=SNpJAAAAMAAJ&redir_esc=y.

[20] D. Powell, D.I. Ma'ruf, y I.Y. Rahman, Practical Considerations in Establishing Corrosion Monitoring for Upstream Oil and Gas Gathering Systems, 2001.

[21] Corrosion inspection and monitoring | Wiley (accedido may 17, 2021), https://www.wiley.com/en-us/Corrosion+Inspection+and+Monitoring-p-9780470099759.

[22] I. R.-C., Undefined 2005, Corrosion Management for an Offshore Sour Gas Pipeline System», *onepetro.Org*, 2005. Accedido: may 07, 2021. [En línea]. Disponible en: https://onepetro.org/NACECORR/proceedings-abstract/CORR05/All-CORR05/NACX10-5638/115522.

[23] C.A. Loto, Microbiological corrosion: mechanism, control and impact—a review, Int. J. Adv. Manuf. Technol. 92 (9-12) (2017) 4241–4252. Springer London.

[24] B. Little, R. R.- Corrosion, y undefined, A Perspective on Corrosion Inhibition by Biofilms, *meridian.allenpress.Com*, 2002. Accedido: may 08, 2021. [En línea]. Disponible en: https://meridian.allenpress.com/corrosion/article-abstract/58/5/424/161318.

[25] C. Sendner, S. Sakong, y A. Groß, Kinetic Monte Carlo simulations of the partial oxidation of methanol on oxygen-covered Cu(110), Accedido: may 12, 2021. [En línea]. Disponible en: https://www.sciencedirect.com/science/article/pii/S0039602806007047.

[26] J. Światowska, et al., Corrosion and passivity of metals in methanol solutions of electrolytes Nepal Project-NouvellEs Protections des ALuminiums View project SiBAT-In situ and Ex situ Spectroscopic Investigations of Electrode Processes on Si-based Anode Materials for Lithium Ion Batteries View project CORROSION AND PASSIVITY OF METALS IN ALCOHOL SOLUTIONS OF ELECTROLYTES, Artic. J. Solid State Electrochem. (2009).

[27] D. Naegeli, P. Lacey, M. Alger, D.E.-S. transactions, y undefined, «Surface corrosion in ethanol fuel pumps», JSTOR (1997). Accedido: may 12, 2021. [En línea]. Disponible en: https://www.jstor.org/stable/44731593.

[28] E. Otero, Corrosión y degradación de materiales, Síntesis, Madrid, 1997. Accedido: sep. 05, 2017. [En línea]. Disponible en: https://scholar.google.es/scholar?hl=es&q=E.+Otero,+Corrosión+y+degradación+de+materiales.+Síntesis,+Madrid+(1997).&btnG&lr&pli=1.

[29] J. De Souza, O. Mattos, L. Sathler, H.T.-C. science, y undefined, Impedance Measurements of Corroding Mild Steel in an Automotive Fuel Ethanol with and without Inhibitor in a Two and Three Electrode Cell, Elsevier, 1987. Accedido: may 03, 2021. [En línea]. Disponible en: https://www.sciencedirect.com/science/article/pii/0010938X87901302.

[30] H. Jahnke, M. Schönborn, Electrochemical corrosion measurements in motor fuels based on methanol and ethanol, Mater. Corros. 36 (12) (1985) 561–566.

[31] Y. Yahagi, Y. Mizutani, Corrosive wear of steel in gasoline-ethanol-water mixtures, Wear 97 (1) (1984) 17–25, ago.

[32] P. Westbrook, Compatibility and Permeability of Oxygenated Fuels to Materials in Underground Storage and Dispensing Equipment, Rep. State Water Resour. Control (1999). Accedido: jun. 21, 2017. [En línea]. Disponible en: http://swrcb2.swrcb.ca.gov/water_issues/programs/ust/leak_prevention/docs/ust_team1_attachment_a.pdf.

[33] J. De Souza, O. Mattos, L. Sathler, y H. Takenouti, Impedance Measurements of Corroding Mild Steel in an Automotive Fuel Ethanol with and without Inhibitor in a Two and Three Electrode Cell, Corros. Sci., 1987. Accedido: sep. 01, 2017. [En línea]. Disponible en: http://www.sciencedirect.com/science/article/pii/0010938X87901302.

[34] L.M. Baena, M. Gómez, y J.A. Calderón, Aggressiveness of a 20% bioethanol-80% gasoline mixture on autoparts: I behavior of metallic materials and evaluation of their electrochemical properties, Fuel 95 (2012).

[35] ASTM G102 - 89(2015)e1 Standard Practice for Calculation of Corrosion Rates and Related Information from Electrochemical Measurements (accedido may 25, 2021), https://www.astm.org/Standards/G102.htm.

[36] M. Stern, A.L. Geaby, Electrochemical polarization», J. Electrochem. Soc. 104 (1) (1957) 56, ene.

[37] M. Stern, E.D. Weisert, Proc. Amer. Soc. Testing - Google Académico, in: https://scholar.google.es/scholar?hl=es&as_sdt=0%2C5&q=Stern%2C+M.+and+ED+Weisert%3A+Proc.+Amer.+Soc.+Testing+Mater.+59+%281959%29%3A+1280&btnG= (accedido may 25, 2021).

[38] J.J. Shim, J.G. Kim, Copper corrosion in potable water distribution systems: influence of copper products on the corrosion behavior, Mater. Lett. 58 (14) (2004) 2002–2006.

[39] A.M. Abdel-Gaber, B.A. Abd-El Nabey, I.M. Sidahmed, A.M. El-Zayady, y M. Saadawy, Effect of temperature on inhibitive action of damsissa extract on the corrosion of steel in acidic media, Corrosion 62 (4) (2006) 293–299, abr.

[40] E. Almeida y M. Morcillo, Corrosión y Protección de Metales en las Atmósferas de Iberoamérica, Parte I: Mapas de Iberoamérica de Corrosividad Atmosférica M, CYTED, Madrid, 1999.

[41] E. Hu, Y. Xu, X. Hu, L. Pan, S. J.-R. energy, and undefined, Corrosion Behaviors of Metals in Biodiesel from Rapeseed Oil and Methanol, Elsevier, 2012. Accedido: feb. 15, 2018. [En línea]. Disponible en: https://www.sciencedirect.com/science/article/pii/S0960148111003922.

[42] R. Kane, J. Maldonado, Stress Corrosion Cracking of Carbon Steel in Fuel Grade Ethanol: Review and Survey, 2003.